Chapter 3
Thermal Fatigue Analysis

Rainer Dudek and Ellen Auerswald

3.1 Introduction

One main reliability concern of the solder joints is related to thermal cycling loading, induced by either environmental temperature changes or active power on/off cycling. Low-cycle fatigue damage can be caused by this type of loading. The main source for thermal fatigue failure is the thermal expansion mismatch of the different materials soldered together, when the assemblies are subjected to a thermal cyclic environment already discussed previously. The most damaging mismatch occurs usually between the component and the printed wiring board (PWB) the component is soldered to, also called "global mismatch". Another kind of mismatch is that between the component and the solder material itself, the so-called "local mismatch". Its importance depends on the size of the solder joints; for current joint sizes, it is gaining importance only for cycle numbers greater than approximately 1000 of the characteristic temperature range −40 to 125°C. The so-called "inner mismatch", occurring between different solder phases and grains, causes solder fatigue also within free-standing solder layers in the absence of any other material. In tin-based lead-free solders, the anisotropic nature of the tin grains has turned out to be the major source for inner mismatch effects [1, 2]. Its effects on the long-term stability of the joints are still an open question.

R. Dudek (✉)
Fraunhofer ENAS, Micro Materials Center Berlin and Chemnitz,
Technologie-Campus 3, 09126 Chemnitz, Germany
e-mail: Rainer.Dudek@enas.fraunhofer.de

E. Auerswald (✉)
Fraunhofer IZM, Micro Materials Center Berlin and Chemnitz,
Volmerstr. 9B, 12489 Berlin, Germany
e-mail: Ellen.Auerswald@izm.fraunhofer.de

G. Grossmann and C. Zardini (eds.), *The ELFNET Book on Failure Mechanisms, Testing Methods, and Quality Issues of Lead-Free Solder Interconnects*,
DOI: 10.1007/978-0-85729-236-0_3, © Springer-Verlag London Limited 2011

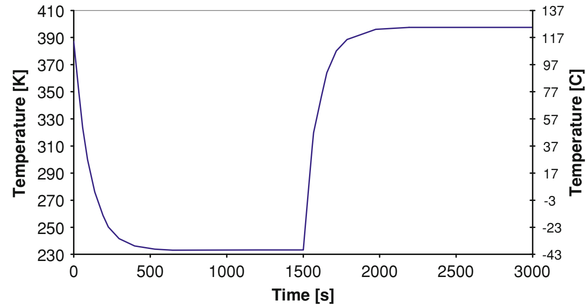

Fig. 3.1 Characteristic test temperature cycle

Two fundamental approaches are available to characterize the solder joint fatigue resistance. The first, which is applied to the majority of electronic products, is thermal test cycling. To achieve comparable statements in a reasonable time, various different test cycles have been defined. They operate usually with higher-temperature cyclic amplitudes and shorter cyclic times compared to the use conditions and are therefore called accelerated tests. Figure 3.1 shows a characteristic temperature versus time function as it occurs at a solder joint during air to air thermal cycling.

Several types of thermal test cycles are available, see Table 3.1. It is important to note that cycling out of use temperature range or with inappropriate high-temperature ramp rates, e.g. liquid to liquid, can engage inappropriate damage mechanisms. Thermal loading also can be dominated by active heating of the devices, i.e. by power cycling. The most complicated temperature-loading conditions occur in those cases when a cyclic temperature environment is overlaid by active heating.

The second approach for characterizing solder fatigue resistance is based on a theoretical fatigue model. Two basic tasks have to be solved by the theoretical model: the first is to define a physical measure to indicate failure, e.g. inelastic strain, or dissipated energy for appropriate strength theories, a damage parameter used in damage theories, or fracture toughness if a fracture mechanical approach is selected. The second task is to link this failure indicator to a critical cycle number.

3.2 Fatigue Failure Mechanism

Because the use temperatures of lead-free solders are also above 0.5 of their melting points (in K), as it was the case for Sn–Pbn solders, creep is a deformation mechanism which is important for materials degradation. Combined with slow loading during the different kinds of thermal cycles, the creep deformation kinetics determines the thermal fatigue behaviour of a solder to a high degree.

Failure of solder joints is a complex sequence of possible failure mechanisms. For conventional Sn–Pb solders, the sequence involves grain/phase coarsening, grain boundary sliding, matrix creep, micro-void formation and linking, and results in macro-crack initiation and crack propagation.

In the case of tin-based lead-free solder joints, the damage accumulation process leads to less well-known mechanisms. It includes thermo-mechanically

Table 3.1 Overview on thermal testing

Thermal testing	Influencing parameters	Methods
Thermal cycling (including thermal shock air to air)	Temperature rate	One-chamber cycling
	Dwell time	Two-chamber cycling
	Temperature extremes	
	Mean temperature	
Thermal shock (liquid/liquid)	Dwell time	Dip in hot and cold liquid
	Temperature extremes	
	Mean temperature	
Power cycling	Inhomogeneous temperature distribution	Power up/down
	Temperature rate	Ambient temperature
	Dwell time	Elevated temperature
	Temperature extremes	
	Mean temperature	

induced recrystallization, voiding and micro-cracking at regions where high induced strains cause local deformations in zones of local strain incompatibilities, e.g. colony or grain boundaries of different nature [3–5]. The micro-cracks tend to nucleate to form a macro-crack, also in dependence on the outer stress field. This behaviour can be related to the strengthening mechanism of Sn-based alloys, which can be seen in the tiny dispersed intermetallic particles embedded in the inherently soft ß-Sn matrix, mainly composed of $AgSn_3$.

During transition, there is also likely to be mixed assembly of both tin–lead and lead-free systems on the same board. The issue was studied by several authors, see e.g. [6, 7].

3.3 Thermal Test Cycling Standards

Because of the high importance of thermal loading in various electronic applications, thermal testing of lead-free solder joints has been studied extensively, see e.g. [8–12]. The accelerated thermal cycling test is a standard procedure to evaluate product reliability.

Currently available standards:

- IPC-9701A, “Performance Test Methods and Qualification Requirements for Surface Mount Solder Attachments”
- IEC/EN 60068 Part 2–14; “Environmental testing-Temperature Change”
- JESD 22-A104, “Temperature Cycling”
- various industry/company internal standards

Table 3.2 Product categories and worst case use environments for surface-mounted electronics (for reference only), cited from IPC-9701 A

Product category (typical application)	Temperature (°C)[a]	Worst case use environment							
	Storage	Operations	T_{min} (°C)[b]	T_{max} (°C)[b]	ΔT (°C)[c]	T (h)[d]	Cycles (year)	Typical years of service	Approx. accept. failure risk (%)
Telecom	−40	−40	−40	85	35	12	365	7–20	0,01
Computer/peripherals	−40	0	0	60	20	2	1460	5	0,1
Commercial aircraft	−40	−40	−55	95	20	12	365	20	0,001
Industrial arid automotive passenger compartment	−55	−40	−55	95	20 &	For all 12	185	10–15	0,1
					40 &		100		
					60 &		60		
					80		20		
Automotive (underhood)	−55	−40	−55	125	60 &	1	1000	10–15	0,1
					100 &	1	300		
					140	2	40		
Consumer	−40	0	0	60	35	12	365	1–3	1

& in addition

[a] All categories may be exposed to a process temperature range of 18–260°C

[b] T_{min} and T_{max} are the operational (test) minimum and maximum temperatures, respectively, and do not determine the maximum ΔT

[c] ΔT represents the maximum temperature swing, but does not include power dissipation effects

[d] The dwell tune to is the time available for the creep of the solder joints during each temperature half-cycle

Table 3.3 Temperature cycling requirements, mandated and preferred test parameters within mandated conditions, cited from IPC-9701A

Test condition	Mandated condition
Cycle condition	
TC1	0°C… +100°C (Preferred Reference)
TC2	−25°C… +100°C
TC3	−40°C… +125°C
TC4	−55°C… +125°C
TC5	−55°C… +100°C
Test duration	Preferred test duration: Until 50% (Preferred 63.2%) cumulative failure or
Number of thermal cycles (NTC)	requirement
NTC A	200 cycles
NTC B	500 cycles
NTC C	1,000 cycles (preferred for TC2, TC3. TC4)
NTC D	3,000 cycles
NTC E	6,000 cycles (preferred for TC1)
Low-temperature dwell	10 min
Temperature tolerance	0°C/−10°C [0°C/+5°C]
High-temperature dwell	10 min
Temperature tolerance	+10°C/0°C [+5°C/0°C]
Temperature rate	≤20°C/min
Full production sample size	>33
Printed wiring (circuit) board thickness	2.35 mm
Test monitoring	Continuous monitoring (event detector preferred)

Since the service conditions differ strongly, no general standard test can be defined for electronic products. A classification for various industries is given in IPC-9701A, see Table 3.2. The variety of thermal test cycles as defined by IPC-9701A is given in Table 3.3.

An overview on the different thermal fatigue testing strategies is given in Tables 3.4 and 3.5.

3.3.1 Fatigue Failure Detection

The occurrence of fatigue failure is detected either by electrical resistance measurements or by visual inspection of the solder joints' cross sections with regard to solder cracking. A third methodology to detect fatigue failure is the shear test, which is limited to simple component geometries, e.g. leadless ceramic components, and becomes very insensitive at states of progressed damage.

The electrical resistance measurement is the simplest technique and allows non-destructive failure detection for a statistically relevant number of components. However, often electrical opens resulting from solder joint failures are intermittent and may be difficult to detect accurately. This issue has turned out to be even more

Table 3.4 Overview on thermal cycling testing

	Slow thermal cycling (air/air)	Thermal shock (air/air)	Thermal shock (liquid/liquid)	Field cycling
Standards	IPC-970A JESD 22-A104	IPC-9710A JESD 22-A104	IEC/EN 60068 Part 2–14	None, company specific
Methods/ Equipment	Place in temperature chamber at varying temperature. One-chamber oven. Hot/cold with air circulation	Move (automatically or manually) between hot and cold chamber/two temperature chambers or a two-chamber oven with air circulation	Dip in hot/cold liquid bathes with heating/ cooling equipment	Power up/down, optionally environmental temp. change/ electrical loading equipment, optionally temperature chamber
Usage	Frequently	Most frequently	Not recommended for solder fatigue, tends to induce failure mechanisms different from the field	Rare
Advantages	Relatively slow, induces best field-related creep-dominated failure. Can be combined with other tests (Vibration, moisture)	Relatively fast, induces field-related creep-dominant failure	Fast. Cheap equipment	Shows field behaviour
Drawbacks	Long testing times, expensive equipment	Expensive equipment	Failure mechanisms different from filed failures	Slow, results device dependent
Influencing parameters	Dwell time, temperature extremes, mean temperature, ramp rates	Dwell time, temperature extremes, mean temperature	Temperature cycling parameters	Temperature cycling parameters, ramp rates, dwell times, gradients in power up/ down

(continued)

Table 3.4 (continued)

	Slow thermal cycling (air/air)	Thermal shock (air/air)	Thermal shock (liquid/liquid)	Field cycling
Coupling to theoretical analysis prediction	Coffin-Manson type empirical laws, FEA (based on secondary creep law and creep strain/ energy dissipation)	Coffin-Manson type empirical laws, FEA (based on secondary creep law and creep strain/ energy dissipation)	FEA (should include coupling of temperature gradients and primary/ secondary creep)	Empirical acceleration factors partially available, FEA (may include coupling of temperature gradients, secondary creep mostly sufficient)

important for lead-free solders than for the tin–lead materials. Whenever possible, online measurements should be preferred to avoid misleading results from the electrical measurements. Moreover, the latter method usually has to be combined with cross sectioning of the joints of interest. An example is shown in Fig. 3.2 for $SnAg_{3.5}$ solder, where in contrast to the totally broken joint, only a slight resistance increase was detected. A second example is shown in Fig. 3.3 for $SnAg_{3.5}Cu_{0.5}$ solder. It can be observed from the figure that cracking of large parts of the joints is not detectable by offline resistance measurement at room temperature. The resistance increases to infinity only if the cracked surfaces really move apart from each other, as shown in Fig. 3.4. Thus, a strict failure criterion is recommended for electrical resistance change, since it is not sensitive to cracking. Ideally, event detectors have to be preferred, as is recommended by IPC-9701A. According to this standard, offline measurement results are not precise enough to detect fatigue failure.

3.4 Theoretical Modelling of Thermal Fatigue

During the last decade, the rapid development of cheap and powerful computer technology has shifted the focus of reliability analysis of solder joints towards the use of finite element analysis (FEA), see e.g. [13–16]. However, since creep is the dominant deformation mechanism of solder, high effort is required to determine the creep properties. Several experimental techniques are in use to determine these creep properties of solders, which are summarized in Table 3.6. Because of the effects of microstructure on the creep behaviour, no unique creep properties seem to exist for both leaded and lead-free solders, i.e., the published properties are sometimes conflicting [14, 17, 18] and the ones used therefore approximate in character. Additionally, the properties-metallurgy dependencies of lead-free solders are still a subject of research [19, 20].

Table 3.5 Overview on thermal test cycling related to different standards

Thermal cycling/ shock	IPC-970A, Feb. 06 Test methods and qualification requirements for SM solder attachments	IEN/EN 60068 part 2–14, 2000 Environmental testing: change of temperature	JEDEC standard JESD 22-A104-A, Dec 1989 temperature cycling	Company-project internal data related to solder fatigue
Temperature rate	Air to air, ≤20°C/min measured at samples (no liquid to liquid)	(a) Fast air to air, defined ramps (b) Slow air to an, defined ramps (c) fast liquid to liquid	Air to air, ≤1 min transfer time, heating of samples within 15 min	<10–30°C/min
Equipment	One (preferred) or two chambers	(a) Two chambers (b) One chamber (c) Two liquid bathes	One (preferred) or two chambers	One of two chambers (preferred), liquid to liquid rarely applied due to the risk to induce irrelevant failure mechanisms
Dwell time	10 min (SnPb) 10 min (SAC) for "stand alone" life assessments, not to compare to SnPb due to slower creep) ≥30 min (creep damage somewhat comparable to SnPb)	(a) Ramp rates 1, 3 or 5°C/min, dwell times 3 h to 10 min (b) Ramp times 2–3 min or 20–30 min or <10 s, dwell times 3 h to 10 min (c) Ramp times 8 s or 2 s, dwell times 20 min to 5 min or 15 s to 5 min	≥10 min	10 min to 2 h

(continued)

Table 3.5 (continued)

Thermal cycling/ shock	IPC-970A, Feb. 06 Test methods and qualification requirements for SM solder attachments	IEN/EN 60068 part 2–14, 2000 Environmental testing: change of temperature	JEDEC standard JESD 22-A104-A, Dec 1989 temperature cycling	Company-project internal data related to solder fatigue
Temperature extremes	−55 to 125°C different combinations, 0–100°C preferred (SnPb, SAC, SnBi), −25 to 75°C SnBi on SnPb plating	(a), (b) Worst case different combinations (c) Characteristic from 0 to 100°C	−65 to 200°C, worst case, different combinations	−55 to 150°C, characteristic −40 to 125°C
Definition of failure	Continuous intermittent event monitoring, ≥1,000 Ω, >1 μs, 10 events, report first event (preferred) and/or continuous intermittent event monitoring, ≤20% increase, max. 5 readings, report average	Loss of device electrical functionality under nominal and worst case conditions, mechanical damage	Loss of device electrical functionality under nominal and worst case conditions, mechanical damage (cracking, chipping, breaking, loss of hemieticity)	Offline measurement (char. ≥50% increase), on line resistance monitoring (char. ≥20% increase), online event monitoring (char. ≥1,000 Ω, >1 μs), cross sectioning (crack progress), shear testing (char. ≥50% load drop)
Recommendation for "pass condition"	Product category dependent (table)	Characteristic (a) 5 cycles (b) 2 cycles (c) 10 cycles	1,000 cycles	Product or test dependent, characteristic 1,000 cycles −40 to 125°C

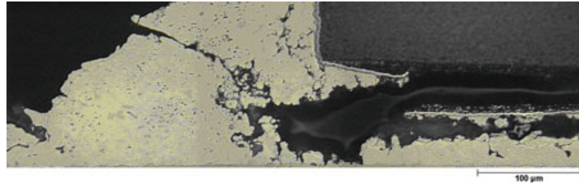

Fig. 3.2 Chip resistors 0805 with SnAg solder on FR-4 PCB after 2,000 cycles −40…125°C, 60 min: resistance increased only by 164 mΩ at room temperature (H. Berek, FnE GmbH, Freiberg)

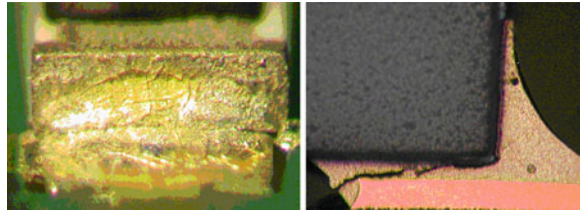

Fig. 3.3 Chip resistors 1206 with SAC solder on FR-4 PCB after 1,000 cycles −40…125°C, 60 min: resistance increased from 26 to 28 mΩ at room temperature (Z. Drozd, Warsaw University of Technology [10])

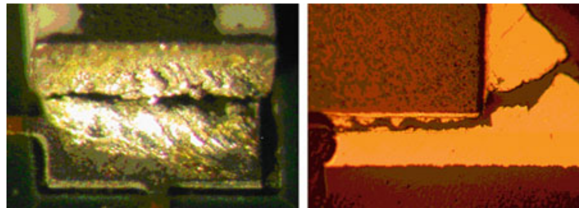

Fig. 3.4 Chip resistors 1206 with SAC solder on FR-4 PCB after 2,000 cycles −40…125°C, 60 min: resistance increased from 26 mΩ to ∞ at room temperature (Z. Drozd, Warsaw University of Technology)

It was already mentioned that the thermal cyclic environment can vary, and that the relation between test cycles and field cycles, the so-called acceleration factors, are of special interest. Simplified analytical models can be very useful in cases to avoid the high effort of numerical modelling. An experimentally supported model for determining the acceleration factor N_{test}/N_{field} for lead-containing solders was developed by Norris and Landzberg [21]. This model was adopted by Pan et al. [22] for SAC387 solders as shown below.

SnPb

$$N_{\mathrm{field}(x)} = N_{\mathrm{test}(x)} \left(\frac{\Delta T_{\mathrm{test}}}{\Delta T_{\mathrm{field}}} \right)^{c1} \left(\frac{f_{\mathrm{field}}}{f_{\mathrm{test}}} \right)^{\frac{1}{3}} \exp\left[1414 \left(\frac{1}{T_{\mathrm{field}}} - \frac{1}{T_{\mathrm{test}}} \right) \right] \tag{3.1}$$

Table 3.6 Overview on solder creep and fatigue characterisation

	Tensile test	Lap shear test with large joint area	Component type laps shear test	Ring- and plug test
Specimens	Macro sized dog bone; miniaturized dog bone	Single/double lap shear with large joint area (Cu on Cu)	Single/double lap shear with component type joints (FC, BGA, LGA)	Copper plug soldered in copper ring subjected to torsional ortensional load; copper wire soldered in via subjected to tensional load
Measuring apparatus	Standard/miniaturized tensile testers; commercially available	Standard/miniaturized tensile testers; commercially available	Special purpose test equipment	Special miniaturized torsion/ tensile testers; weights
Usage	Frequently; creep characterization; fatigue characterisation; includes a high risk of buckling effects	Most frequently; creep characterization; fatigue characterisation	Rare; creep characterization; fatigue characterisation	Rare; creep characterization; fatigue characterisation; creep characterization only
Advantages	Simple specimens with high precision; microstructure can be controlled by temperature regime; easy to measure/high precision; one-dimensional stress state	Interaction with pad finishes, alloying content and intermetallics match real joints; high joint size precision difficult; volume comes close to real joints;shear loading is dominant joint loading	Interaction with pad finishes, alloying content and intermetallics match real joints; volume matches real joints; shear loading is strongly overlaid by three-dimensional stress state	Volume comes close to real joints/matches real joints; shear loading is dominant joint loading (both wire and plug); simple measurement
Drawbacks	Missing interaction with pads (alloying effects, intermetallics); volume large related to actual joints, even for miniaturized specimens	Almost pure shear for large joints, but loss of joint matchdifficult to process with high precision; cooling regime/microstructure can differ from joint	Multi-dimensional stress state for small joints (FEA required); difficult to measure with high precision	Strain gradient and multidimensional stress state can beimportant (FEA required, both wire and plug); difficult to process with high precision

(continued)

Table 3.6 (continued)

	Tensile test	Lap shear test with large joint area	Component type laps shear test	Ring- and plug test
Major sources of errors	Strain measurement; microstructure is not characteristicfor joint	Dwell time, temperature extremes, mean temperature	Temperature cycling parameters	Temperature cycling parameters, ramp rates, dwell times,gradients in power up/down
Specimens	Macro sized dog bone; miniaturized dog bone	Coffin-Manson type empirical laws, FEA (based on secondarycreep law and creep strain/energy dissipation)	FEA (should include coupling of temperature gradients and primary/secondary creep)	Empirical acceleration factors partially available, FEA (mayinclude coupling of temperature gradients, secondary creep mostly sufficient)

SAC 387

$$N_{\text{field}(x)} = N_{\text{test}(x)} \left(\frac{\Delta T_{\text{test}}}{\Delta T_{\text{field}}}\right)^{2.65} \left(\frac{t_{\text{test}}}{t_{\text{field}}}\right)^{0.136} \exp\left[2185 \left(\frac{1}{T_{\text{field}}} - \frac{1}{T_{\text{test}}}\right)\right] \tag{3.2}$$

$N_{\text{field}}(x)$, number of field cycles at which a percentage x of connections has failed, for example, $N_{\text{field}}(50)$ = mean cycles to failure at which 50% of connections have failed; $N_{\text{test}}(x)$ analogous number of test cycles; c_1, empirical constant, applicable is $c_1 = 1.9$ for SnPb; f cycling frequency expressed in number of cycles/day; t dwell times (equal dwell times for hot and cold dwell preferred); T maximum cycling temperature in K.

However, because of the complicated dependencies of SAC solder on various effects like type of components, metallization and joint size, the derived equation seems questionable [23]. The SnPb constants for the Norris–Landsberg model seem to be a better fit to the existing Pb-free data than the revised constants provided in the paper by Pan et al. Further work is required with respect to the eutectic SAC solder compositions and those improved by spurious alloys.

3.5 Open Questions

- Long-term fatigue performance of different lead-free solders in field use in dependence on the component type and adequate formulation of acceleration factors;
- Reliability of different lead-free solders under the combined action of different leadings, e.g. low-cycle fatigue overlaid by vibration;
- Effects of spurious alloys on the creep and thermal fatigue performance of second-generation lead-free solders;
- Development of virtual reliability design methodologies, aiming at relations between test cycling and mission profiles for use in high-reliability applications for low-cycle fatigue loadings and for combined loadings;
- Materials characterization and modelling of second-generation lead-free solders including SnZn, Bi-containing solders, under-eutectic SAC solders with Ni and other spurious alloys, and nanoparticle-containing solders or adhesives. Consideration of miniaturization-related effects on materials properties and modelling, respectively, e.g. the shift of plastic-creep properties of tiny interconnects that approach the meso-structure size (e.g. grain size, primary intermetallics size). Application of nano-indentation techniques towards elastic–plastic, elastic-creep or viscoelastic strongly localized materials characterization, also at thin-film materials or intermetallics;
- Development of sophisticated modelling techniques including viable ones for the meso-structure of materials and damage progress.

References

1. Bieler TR, Jiang H, Lehman LP, Kirkpatrick T, Cotts EJ (2006) Influence of Sn grain size and orientation on the thermomechanical response and reliability of Pb-free solder joints. In: Proceedings, 56th electronic components & technology conference, San Diego, pp 1462–1469
2. Gong J, Liu Ch, Conway PP, Silberschmidt VV (2006) Grain features of SnAgCu solder and their effect on mechanical behavior of micro-joints. In: Proceedings of 56th electronic components & technology conference, San Diego, pp 250–257
3. Dunford S, Canumalla S, Viswanadham P (2004) Intermetallic morphology and damage evolution under thermomechanical fatigue of Pb-free solder interconnections. In: Proceedings of 54th ECTC, Las Vegas, pp 726–735
4. Grossmann G, Jud PP, Sennhauser U (2005) Microstructure and deformation behavior of SnAg3.8Cu0.7 lead-free solder. In: The world of electronic packaging and system integration. Fraunhofer Institute Reliability and Microintegration, Berlin
5. Dudek R, Faust W, Gollhardt A, Michel B (2006) A FE study of solder fatigue compared to microstructural damage evaluation by in situ laser scanning and FIB microscopy. In: Proceedings ITherm 2006, San Diego, USA
6. Dušek M, Nottay J, Hunt C (2001) Compatibility of lead-free solders with PCB materials. National Physical Laboratory, UK, NPL Report MATC (A) 89
7. Clech J-P (2004) Lead-free and mixed assembly solder joint reliability trends. IPC Printed Circuits Expo®, SMEMA Council APEX, Designers Summit 04
8. Andersson et al (2004) Effect of different temperature cycle profiles on the crack propagation and microstructural evolution of lead free solder joints of different electronic components. In: Proceedings of Eurosime, Brussels
9. Schubert A, Dudek R, Auerswald E, Gollhardt A, Michel B, Reichl H (2003) Fatigue life models for SnAgCu and SnPb solder joints evaluated by experiments and simulation. In: Proceedings of 53rd electronic components & technology conference, pp 603–610
10. Drozd Z (2006) Testing methodology and results from thermal shock tests in the project GreenRoSE. ELFNET Project meeting, Athens
11. Vandevelde B, Ratchev P, Limaye P (2006) Latest results from ALSHIRA. ELFNET Project meeting, Athens
12. Dušek M (2006) NPL—lead-free projects of electronics interconnection group. ELFNET Project meeting, Dubendorf
13. Vandevelde B, Gonzalez M, Limaye P, Labie R, Ratchev P, Vanfleteren J, Beyne E (2004) Leadfree solder joint reliability estimation by finite element modelling: advantages, challenges and limitations. In: IPC-/JEDEC 7th international conference on leadfree electronic components and assemblies, Frankfurt
14. Dudek R (2006) Characterization and modelling of solder joint reliability. In: Zhang GQ, van Driel WD, Fan XJ (eds) Mechanics of microelectronics. Springer Science+Business Media, Dordrecht, pp 377–466
15. Lau J, Dauksher W, Vianco P (2003) Acceleration models, constitutive equations, and reliability of lead-free solders and joints. In: Proceedings, 53rd electronic components & technology conference, pp 229–236
16. Zhang Q, Dasgupta A, Haswell P (2003) Viscoplastic constitutive properties and energy-partitioning model of lead-free Sn3.9Ag0.6Cu solder alloy. In: Proceedings of 53rd electronic components & technology conference, pp 1862–1868
17. Clech JP, Handwerker C (2002) Review and analysis of lead-free solder material properties BGA, Flip-Chip. ESPI Inc., NIST
18. Pang JHL, Xiong BS, Neo CC, Zhang XR, Low TH (2003) Bulk solder and solder joint properties for lead free SnAgCu solder alloy. In: Proceedings of 53rd electronic components & technology conference, pp 673–679

19. Wiese S, Meusel E, Wolter K-J (2003) Microstructural dependence of constitutive properties of eutectic SnAg and SnAgCu solders. In: Proceedings of 53rd electronic components & technology conference, pp 197–206
20. Wiese S, Roellig M, Mueller M, Rzepka S, Nocke K, Luhmann C, Kraemer F, Meier K, Wolter K-J (2006) The influence of size and composition on the creep of SnAgCu solder joints. In: Proceedings ESTC, Dresden, Germany, pp 912–926
21. Norris KC, Landzberg AH (1969) Reliability of controlled collapse interconnections. IBM J Res Dev, pp 266–271
22. Pan N, Henshall GA, Billaut F, Dai S, Strum MJ, Benedetto E, Rayner J (2005) An acceleration model for Sn-Ag-Cu solder joint reliability under various thermal cycle conditions. In: Proceedings of SMTA international conference, Chicago
23. Hillman C (2006) Assessment of Pb-Free Norris-Landzberg model to JG-PP test data. Presentation DfR Solutions